Comparison of LCC/VSC-HVDC systems for power/frequency control in interconnected grids

Francesco Puddu
Dept. of Electrical and Electronic Engineering
University of Cagliari
Cagliari, Italy
f.puddu56@studenti.unica.it

Emilio Ghiani
Dept. of Electrical and Electronic Engineering
University of Cagliari
Cagliari, Italy
emilio.ghiani@unica.it

Gianni Celli
Dept. of Electrical and Electronic Engineering
University of Cagliari
Cagliari, Italy
gcelli@unica.it

Roberto Gnudi
Strategy, Development and Dispatching
Terna S.p.A.
Roma, Italy
roberto.gnudi@terna.it

Giorgio Maria Giannuzzi
Strategy, Development and Dispatching
Terna S.p.A.
Roma, Italy
giorgio.giannuzzi@terna.it

Fabrizio Pilo
Dept. of Electrical and Electronic Engineering
University of Cagliari
Cagliari, Italy
fabrizio.pilo@unica.it

***Abstract*—The increasing complexity of interconnected power systems, combined with the growing integration of renewable energy sources, poses critical challenges for maintaining frequency stability. HVDC links represent a promising solution for enabling controlled power exchange and coordinated regulation between asynchronous grids. This paper aims to compare the two dominant HVDC technologies, Line Commutated Converter and Voltage Source Converter, with a particular focus on their ability to provide ancillary services to the power system. A MATLAB Simulink model, related to an asynchronous interconnected system where and HVDC system is involved, has been developed, and its control system has been implemented and simulated in order to verify the HVDC's capability to respond to various kinds of grid disturbances. Results show that the two HVDC technologies offer similar performance in terms of response time and frequency stability, even though the VSC system outperforms traditional LCC setups in terms of flexibility and general adaptability under varying grid conditions.**

Keywords— HVDC, LCC, VSC, asynchronous grid, power-frequency control

I. INTRODUCTION

Modern power systems, which are increasingly oriented towards the integration of massive amounts of renewable energy plants, are facing increasing problems related to grid security and market integration within and between neighboring states, suffering in particular from the saturation of available transit capacity. To solve these issues, Transmission System Operators (TSOs) in Europe are increasingly investing in strengthening and modernizing their networks to unblock congested corridors and maintain sufficient flexibility in controlling energy flows. In fact, under standard operating conditions of multiple interconnected power systems, active power exchanges across tie lines are determined according to regulations on power flow and load frequency control between areas, along with market dynamics, all while respecting grid constraints. From the point of view of the individual operator of an electrical system, interconnected systems can be seen as one dominant power system. When a disturbance occurs within the external interconnected system, the resulting frequency transients also affect the power exchange values, causing deviations from the programmed values and/or local imbalances. Each independent power system typically uses a centralized controller that generates a signal proportional to the integral of the frequency deviation and the power deviation at the interconnection. This signal is then sent to generation units enabled to provide power/frequency regulation within the same network, with the aim of restoring the power flow to its scheduled value. This signal, or a fraction of it, can also be sent to a production unit (PU) located in an asynchronous system, one connected to the main AC system via an HVDC link. With current control methods, such a unit would adjust its operating point based on the regulation request, causing a frequency deviation in the isolated system. The HVDC system would then respond through its primary frequency controller, adjusting power flow proportionally to the frequency variation until internal resources restore balance. However, under this configuration, the asynchronous reserve cannot provide continuous regulation, since the HVDC system lacks the capability to follow the control signal, thus changing its operating point indefinitely. This lack of coordination can result in unacceptable frequency deviations in the asynchronous system. Conversely, if both the asynchronous reserve and the HVDC system receive the same control signal and follow an identical power ramp, the service could be delivered in a coordinated way, minimizing frequency disturbances. The key benefit of this approach is the possibility to open new regulation markets to Independent Power Producers (IPP) in asynchronous systems, expanding service availability and revenue opportunities. This effectively removes location-based constraints, allowing isolated units to contribute to external system control, and ultimately enhancing overall system flexibility and market efficiency.

This paper is structured as follows: a brief comparison of HVDC system technologies will highlight the main differences between LCC and VSC systems, with a focus on Frequency Restoration Reserve (FRR) capabilities. The Simulink environment wherein the simulations are conducted will be subsequently shown, the models of AC power systems and HVDC systems will be discussed as well as their control systems. Next, the simulation results will be presented, followed by a final analysis aimed at determining the overall

operating ranges of HVDC technologies engaged in FRR services.

II. LCC AND VSC HVDC SYSTEMS

In the arena of HVDC power transmission, two main technologies are primarily used for power conversion: Line-Commutated Converters (LCC) and Voltage Source Converters (VSC). The LCC technology, regarded as the more established and traditional approach, is based on the use of line-commutated converters employing thyristor valves. In contrast, the VSC technology, which is more recent and innovative, utilizes insulated gate bipolar transistors (IGBTs), allowing for more flexible power flow control and greater adaptability to weak or isolated grids. For instance, reference [1] outlines the general differences between LCC and VSC HVDC systems, highlighting their different power ratings, control techniques and efficiency.

Compared to a VSC system, an LCC system exhibits two main weaknesses when specifically analyzed within the scope of FRR operations. The first weakness concerns the requirement of a minimum power transfer from the converter for proper operation. Operating at significantly reduced power levels would result in high ignition angles, thus requiring the use of increasingly reduced overlap angles [2]. This condition can compromise the safe operation of the valves. In general practice, as in this comparison, the technical minimum power threshold for an LCC system is typically set at 0.10 pu. The second disadvantage of LCC technology lies in the operational burden associated with power reversals across the link, particularly due to the stress imposed on the dielectric insulation of the transmission lines. Unlike VSC systems, in which the power flow can be reversed without altering the link's polarity, an LCC system requires the inversion of the system's polarity to reverse the power flow, resulting in high electrical stress. Power reversal can be performed over different time scales. In the case of a fast power reversal (FPR), polarity inversion is typically completed within one second. Alternatively, the system can be allowed a relaxation period of several minutes during which the voltage is null. In this latter approach, the voltage across the link is first rapidly brought to zero and only after the relaxation period is it raised to the opposite maximum value. The longer the relaxation time, the smaller the residual charge in the insulating material at the moment of polarity inversion, thereby reducing the intensity of the electric field to which the dielectric is subjected. Ref. [3] concludes that performing one FPR per month is sufficient to reduce the lifetime of the insulation by up to 10%, while one FPR per day can reduce the expected lifetime by up to 60%. The same number of polarity reversals can be performed more slowly: for example, a relaxation time of 10 minutes can limit the lifetime reduction to 40%. For longer relaxation times, the reduction of the life loss is progressively smaller, with the most effective changes occurring within the first 20 minutes. For these reasons, power flow reversal in an LCC system must be used sparingly, particularly in its fast variant. During the lifespan of an LCC system, the FPR can only be performed a limited number of times and should be reserved for emergency situations. In the context of secondary frequency control, which is characterized by time scales in the order of a few minutes, power reversal in an LCC system would impose significant electrical stress and consequently cause a significant loss of life in the transmission infrastructure. Therefore, power reversal is not recommended in this application. Due to the two limiting factors described above, the operational flexibility of an LCC system is considerably narrower than that of a VSC.

III. SYSTEM MODELING AND CONTROL

A. AC High Voltage Transmission Systems

All models presented in this paper have been created using Simulink's Specialized Power Systems (SPS) toolbox. The final models used for this work require three distinct 230 kV, 50 Hz AC systems. The dominant AC system wherein the disturbances will occur has an installed capacity of 10000 MW and is modeled through its equivalent circuit, made up of a generator and a resistive load. The same can be said for the continental AC system with 60 GW of installed capacity. The two AC systems are connected via a singular, 100km tie line, thus they are synchronous under standard operating conditions. In addition, the dominant AC system is connected to a smaller, asynchronous AC system through an HVDC link that can either be of the LCC or VSC type depending on the scenario. The type of HVDC system used affects the installed capacity of the asynchronous AC system, being 1300 MW for the VSC case and 4000 MW for the LCC case, the reason for these differences in power rating depending on the HVDC system will be explained timely. The single line diagram of the interconnected AC systems is shown in Fig. 1. In the simulation developed, the HVDC transmission system has been also coupled with a 200 MW Battery Energy System Storage (BESS) interfaced with the grid through a static power converter. The BESS is part of the asynchronous system's Frequency Containment Reserve (FCR), thus can aid in its primary frequency control operations. Of the three PUs present in the asynchronous system, only G1 and G2, both with a rated power of 400 MW, are part of the FCR and FRR, whereas G3, with a rated power of 500 MW, operates at a fixed power level. All the PUs included in the final model are comprised of a salient pole rotor synchronous generator, a control system with an Automatic Voltage Regulator (AVR) and Automatic Generation Control (AGC), an auxiliary resistive load equivalent to 10% of the PU's rated power, and a 13.8/230 kV step-up power transformer. As far as the primary frequency regulation is concerned, all PUs that supply the FCR across all AC systems are equipped with a speed regulator operating with a 5% droop characteristic, in accordance with [4]. The BESS is modeled via a three-phase dynamic load for model simplicity, this element of the SPS library allows for generation or consumption of a set amount of active and reactive power, which can be determined through a vector signal. The controller associated with the BESS enables it to operate at a defined setpoint and to participate in primary frequency control through Frequency Sensitive Mode (FSM) and Limited Frequency Sensitive Mode Under/Over (LFSM-U, LFSM-O). The controller is implemented in compliance with [4] [5], thus can also allow for Reserve Mode (RM) operation if the appropriate State of Charge (SOC) range is exceeded. PUs that supply the FRR of either AC system can change their operating point indefinitely by tracking a signal generated by a centralized controller.

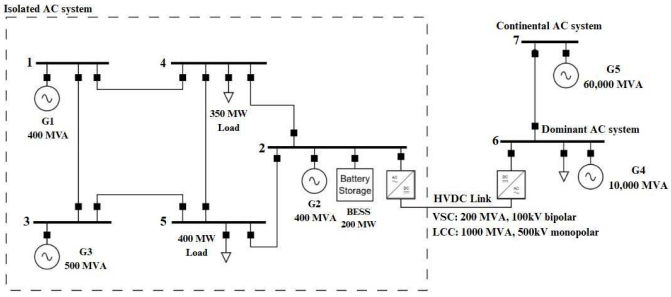

Fig. 1. Single-line diagram of the overall simulated system

Each AC system is considered as a separate control area, thus equipped with its own central control.

The asynchronous area controller outputs a signal that is proportional only to the integral of the difference in frequency with respect to the nominal value of 50 Hz, whereas the controllers associated with the remaining systems will also need to account for the deviation in active power exchange across the tie line.

All controllers are of the integral type, with an integral coefficient k_i high enough to restore the frequency and tie line power flow values within a few seconds after the disturbance. The time scale of the frequency control is thus greatly accelerated due to computational power constraints. The output of the dominant system's controller will generally be referred to as command signal, which is relayed to the dominant system's generator as well as the HVDC system and the BESS situated in the asynchronous area. Only a certain percentage of the command signal is received by both the BESS and HVDC system, as the rest will be relayed to the dominant system's generator. The percentage of the command signal that is assigned to the FRR of the asynchronous area can be established at the beginning of the simulation, however, this parameter may need to be overwritten by a lower value in the event that either the HVDC or the BESS cannot provide the scheduled power due to constraints caused by the combination of their current operating points. The maximum percentage of the command signal that can be assigned to the FRR of the asynchronous area is a function of both BESS and HVDC system's power setpoint, as well as their power limits and the direction in which the power flow variation needs to be executed. For this reason, the command signal is equipped with a signal limiter that changes the secondary regulation band depending on the sign of the command signal. Any excess percentage of the command signal that cannot be covered by the FRR of the asynchronous area will therefore be relayed back to the dominant system's generator.

B. HVDC Systems

Two separate models are required for the simulations, one with each of the HVDC technologies. The base models were initially obtained from [6] and were modified properly for the purposes of this work.

1) VSC system

The base model of the chosen VSC system as well as its control is described by [6]. It represents a VSC-based point-to-point bipolar link with a rated power of 200 MVA. The link operates at a nominal voltage of 100 kV and a nominal pole current of 1 kA. The sinusoidal Pulse Width Modulation (PWM) scheme employed for system control features a frequency modulation index of 27. Consequently, the carrier signal frequency, as well as the switching frequency of the IGBTs, is 1350 Hz, while the frequency of the modulating signal is, as expected, 50 Hz. The two converter stations are connected by two 300 km pole lines. Both converter stations are equipped with their own local control system. These control systems are identical and operate independently, without communication between them. Regardless of whether a station is operating in rectifier or inverter mode, it possesses two degrees of freedom and is therefore capable of regulating one quantity between active power flow and DC-side voltage via the direct component of the current, and one quantity between reactive power flow and AC-side voltage via the quadrature component of the current. The model under consideration does not include an AC voltage regulator, as it is designed solely for interconnection with non-passive grids. Within the simulation environment, it is also possible to designate which converter station acts as the Master and which as the Slave. For each simulation carried out, the converter station located on the asynchronous area is assigned the role of active power controller. This choice ensures optimal coordination between the converter station and the BESS, thus preventing power losses in the transmission systems from producing a net power variation on the asynchronous grid, which could adversely affect frequency stability. The control system computes the three-phase reference voltages to be supplied to the PWM modulator in order to match the assigned setpoints for active power, voltage, and reactive power. All main modifications to the model are applied to the input related to the power reference. The power command is given by the sum of the power setpoint, the primary frequency control response, as well as the command signal percentage assigned to the asynchronous area by the dominant system's controller. The primary frequency control outputs a power response that is proportional to the frequency disturbance following a 1% droop characteristic. To ensure the stability of the primary frequency control, the frequency measurement is taken by a mobile average with a sampling time of 100ms.

2) LCC system

The description of the base model of the LCC-HVDC and its control system is given by [7]. The model in question is a 1000 MW, 500 kV LCC monopolar link. The converter stations are separated by a 300 km line. Both converter stations consist of a three-winding converter transformer and a twelve-pulse thyristor bridge. The converter transformer on the rectifier side features a Yg-connected winding on the AC grid side, with a nominal voltage of 500 kV. The two secondary windings, on the converter side, are configured as Y and D1. As a result, the voltages on the secondary winding with D1 configuration will lag by 30° with respect to those on the Y-connected winding. The nominal secondary voltage is 200 kV. The nominal power rating of the transformer is 1200 MVA, which corresponds to the maximum transmittable power of the link when operating at the technical current limit of 1.2 pu. The transformer configuration at the inverter station is analogous, with a nominal primary voltage of 345 kV. The twelve-pulse converter bridge is obtained by connecting in series two six-pulse bridges. Snubber circuits are connected in parallel to the thyristors, with resistance values of 2000 Ω and capacitance of 0.1 μF. The internal resistance of the diode during conduction is set to 1 mΩ. The pulses vector that activates each bridge is generated by the converter station's pole control. The station's pole control determines the value of the ignition angle α based on the reference current command in the case of the rectifier station, whereas the inverter station works in Constant Extinction Angle (CEA) mode. Each pole control receives the appropriate current

command from a common master control. To better suit the model for the objective of this paper, it was subjected to the modifications below described.

The master control has been modified to operate based on a power command rather than a current command.

- The current reference signal to be sent to the pole control of each converter station is determined through a divider that calculates the ratio between the power command and the rated voltage of the link.
- The sign of the current command is independent of that associated with the power command and is kept constant, while the polarity of the link and the operating mode of the converter station vary accordingly.
- The base model does not allow for power reversal during the simulation. This functionality has therefore been introduced here, allowing the parameters of the converter stations to change dynamically according to the power command.
- The LCC system has been connected to the two previously mentioned AC systems. To enable this connection, transformers are placed at the Point of Common Coupling (PCC) between the HVDC system and the AC grids.

Given the susceptibility of LCC systems to commutation failures caused by disturbances in the AC systems, they must be connected to sufficiently strong AC grids. The most commonly used parameter to determine appropriate operating conditions for an LCC system connected to an AC network is the short-circuit ratio (SCR), calculated as the ratio between the short-circuit power of the AC system at the PCC and the rated power of the HVDC system. An SCR of two is generally considered the minimum requirement for stable HVDC system operation. AC systems with an SCR lower than three are defined as weak systems [2] [8]. To ensure the stable operation of the HVDC system in question, the installed capacity in the asynchronous system has been set to 4000 MW. For simplicity, the entire power increase has been allocated to PU G2.

The original model was based on a fixed-step solver. This has been replaced with the same solver used in the simulations involving the VSC system. The solver employed is the ode45 method with variable-step time discretization. The same power command structure employed for the VSC system is replicated in the LCC power controller. Both HVDC systems elaborate the command signal through a 100 MW/s power ramp, the same is valid in the case of the BESS. PUs on the dominant system also respond to the command signal via a power ramp with similar dynamic.

IV. Results

A. *Performance of VSC-HVDC coordination with the FRR*

The first simulation will analyze the following scenario: at T=3s a 1000 MW load will be connected to the dominant AC system. At the time of the disturbance, the dominant AC system is set to export 1000 MW to the continental grid through its tie line. As the load connects, the power demand within the dominant system suddenly increases, leading to a drop in the system's frequency and a reduction of the tie line power flow. Consequently, the dominant system's central regulator will output a signal that is both proportional to the integral of the frequency variation and the difference in active power exchange with respect to the established value. 90% of the signal is sent to PUs located in the dominant system. The remaining 10% is relayed to both the VSC-HVDC converter station in the asynchronous area and the BESS. The simulation is carried out under the premise of perfect coordination between the two systems, meaning that they will receive the command signal at the same time and will elaborate it through the same power ramp, any desynchronizations among the two systems, either due to time delays or differences in power ramp will lead to disturbances to the asynchronous system's frequency. Before the disturbance occurs, the VSC-HVDC setpoint is set to 0.20 pu, corresponding to a power export from the asynchronous area to the dominant one, whereas the setpoint of the BESS is set to 0.25 pu, meaning that it is currently in a state of discharge. The results of the simulation are presented in Fig. 2. As the command signal increases, both the BESS and the VSC-HVDC system change their operating point simultaneously, following a 100 MW/s power ramp.

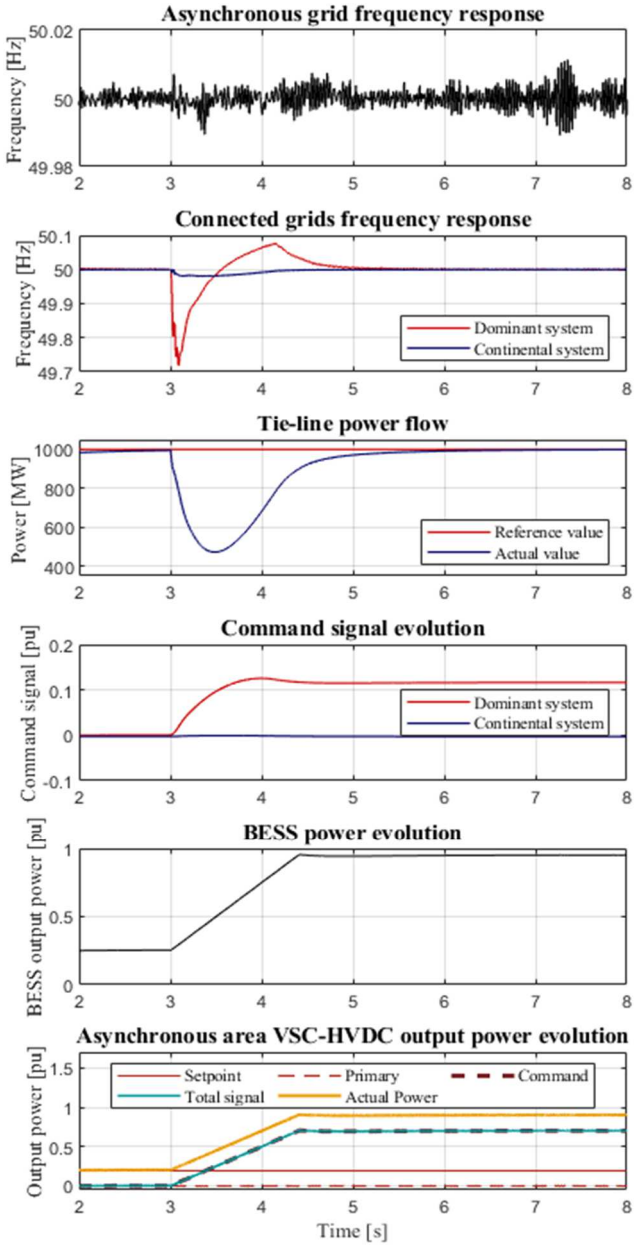

Fig. 2. Coordination between the VSC-HVDC system and the asynchronous area's BESS

Under perfect coordination, the BESS is instantly able to compensate for the additional power absorbed by the HVDC system, leading to no frequency disturbances. In these conditions, the dominant system is able to restore standard operating conditions within 3s from the initial disturbance, while preserving the stability of the asynchronous area. It is also possible to notice how the BESS and HVDC systems' power output is unable to catch up with the command signal in the initial stages of the response, this is due to the power ramp being too shallow. This causes a slight oscillation in the command signal evolution, as well as the frequency response of the dominant AC system. A shallower power ramp exacerbates this effect, however, this behavior should not present itself in an environment featuring a more realistic time scale, as the controllers' time constants would be much higher.

B. Performance of LCC-HVDC coordination with the FRR

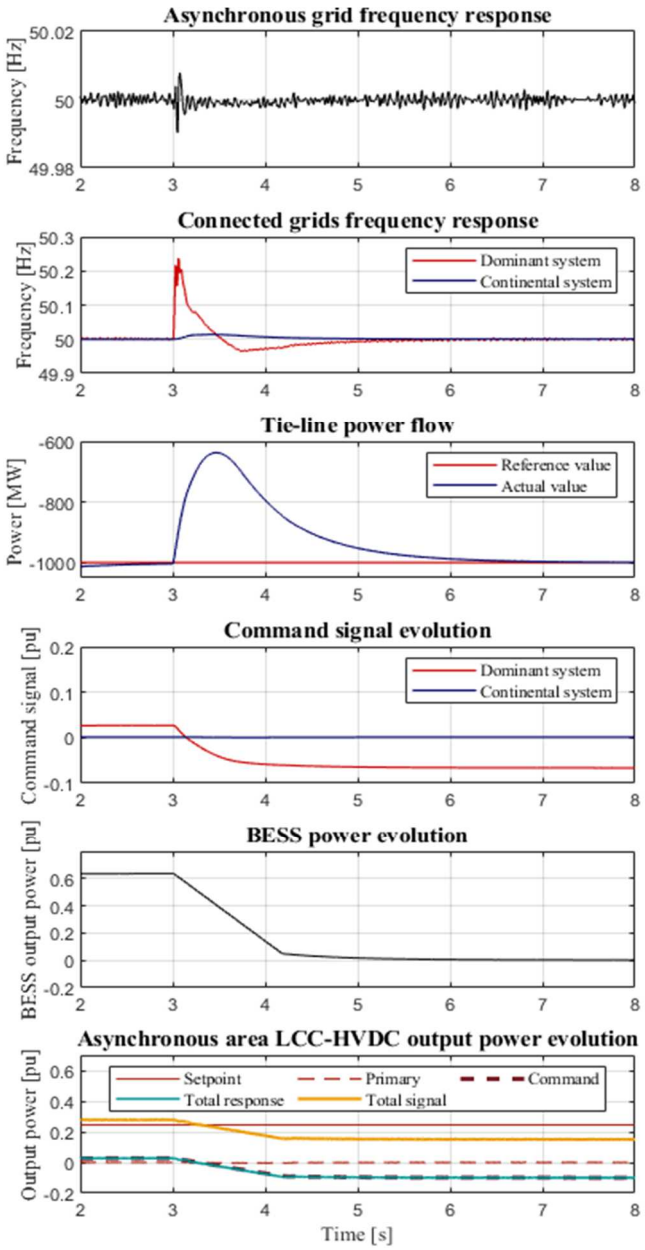

Fig. 3. Coordination between the LCC-HVDC system and the asynchronous area's BESS

A similar scenario is set up for the LCC-HVDC system. At T=3s, a 1000 MW load will be disconnected from the dominant AC system, which is currently set to import 1000 MW from the continental AC system. A spike in frequency and a reduction in tie line power flow are expected. However, the percentage of command signal that is relayed to the FRR of the asynchronous area is purposely set to 20%, meaning that both the BESS and LCC-VSC systems will need to change their operating points by 200 MW. As shown in Fig. 3, the BESS, having an initial setpoint of 0.60 pu, is able to respect the controller's request. However, the LCC system's setpoint of 0.25 pu does not allow the operating point to move below 0.10 pu, which is the system's minimum power requirement. The operating conditions of the two systems are considered by the centralized controller of the dominant system, which determines their asymmetric secondary reserve band. The appropriate limit on the percentage of command signal is imposed as a function of the sign of the command signal itself. As a result, the controller is able to overwrite the set signal percentage, and reduce its value from 20% to 15%, preventing the HVDC system from saturating its operating point to 10%. The remaining 5% will be subsequentially added to the percentage supplied by the dominant AC system's generator. Through this control method, though the request from the dominant system is partially respected, the asynchronous system's frequency remains stable, and the LCC-HVDC system is prevented from operating under unfavorable conditions. It is also to be noted that this scenario would instead pose no problems with the VSC setup, as it doesn't present any minimum power requirements for operation, it is therefore deducible that the VSC system detains an advantage over its LCC counterpart in terms of being available to provide secondary regulation. With the purpose of determining the scale of such advantage, a final iterative analysis is carried out.

V. HVDC SYSTEMS FLEXIBILITY COMPARISON

The objective of this comparison is to quantify the operating range of both HVDC systems and assess the extent of the VSC system's operating range margin over an LCC system of equal nominal power for the provision of secondary frequency control. The comparison is conducted through an iterative analysis, in which only relative power values are considered.

For each of the HVDC systems, a power setpoint is defined. Subsequently, a power variation is imposed, representing the command signal for secondary regulation, the combination of a power setpoint and a requested power variation constitutes one scenario within the analysis. The power request can vary linearly from -2 pu to 2 pu. It is applied in discrete steps, and for each applied demand, the corresponding new power setpoint of the system is computed. If the new setpoint falls within the operating range of the system, the delivery of secondary control service is executed without the intervention on the signal limiter, and thus is considered feasible for that specific scenario. For the VSC system, the operating range is continuous and extends from -1 pu to 1 pu. Conversely, the LCC system features an operating range that is limited from 0.10 pu to 1 pu. A discontinuous operating range, also including the interval from -0.10 pu to -1 pu, is not considered, since polarity reversal in the context of secondary frequency control is deemed unacceptable.

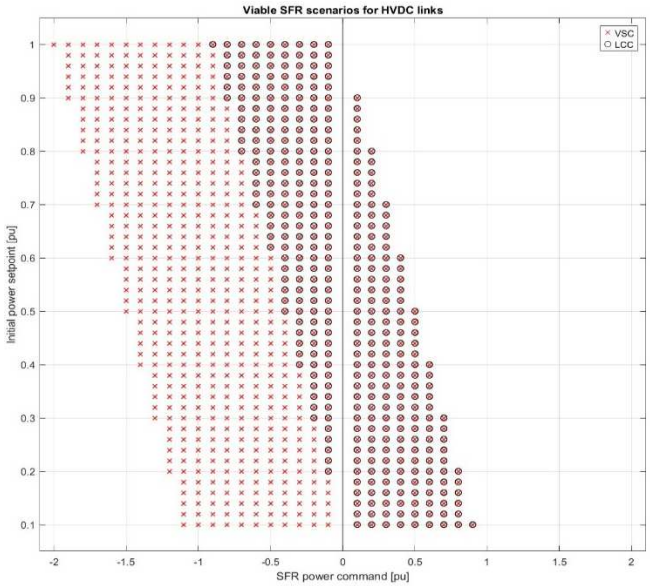

Fig. 4. HVDC systems comparison for secondary control, with power setpoint parity

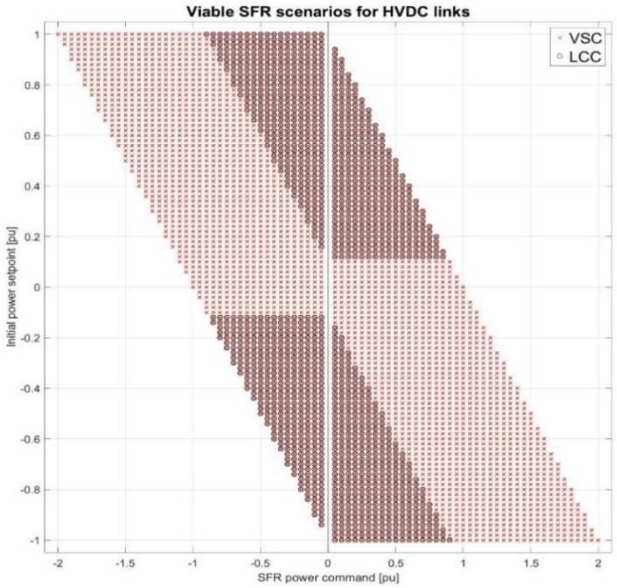

Fig. 5. HVDC systems comparison for secondary control, with all available power setpoints

Additionally, for each scenario, the power margin held by the VSC compared to the LCC is calculated; in cases where the LCC system is unable to provide the service, this margin is greater than zero. The analysis is repeated for increasing initial setpoints ranging from 0.10 pu to 1 pu, with a discretization step of 0.02 pu for both HVDC systems. The power demand is discretized with a step size of 0.1 pu. Initially, the analysis is carried out under equal amount of setpoints. Out of a total of 1886 scenarios analyzed, the VSC system can deliver the service in 930 scenarios, whereas the LCC system is available only in 432 instances. At the end of the analysis, the calculated power margins are used to determine their average value, which is found to be 1.01 pu. Under equal setpoints, the VSC system demonstrates an operational range twice as wide as that of the LCC system. The same results are graphically illustrated in Fig. 4. This figure shows, on the vertical axis, the increasing values of the power setpoint and, on the horizontal axis, the imposed power demand. Given the discrete nature of the analysis, it is possible to identify the individual scenarios in which the regulation service is deliverable. A scenario where the VSC system can provide the service is marked with a red cross, whereas a black circle indicates the same for the LCC system. For each setpoint, the asymmetrical band within which the system can shift its operating point is clearly shown. For positive power demands, both systems are constrained by the same maximum limit. However, for negative demands, it can be observed that the VSC system exhibits a band approximately twice as wide as that of the LCC, thanks to its continuous operating range and its capability to reverse the power flow without compromising the infrastructure's integrity. A similar analysis can be carried out including all possible setpoints, while still disallowing power reversal for the LCC system. The corresponding graphical result, which is coherent with the findings of the previous analysis, is shown in Fig. 5.

VI. Conclusion

This paper aims to compare the two dominant HVDC technologies, LCC and VSC systems for HVDC transmission systems in managing power exchange and coordinated regulation between asynchronous grids.

Simulation results confirm the effectiveness of the LCC and VSC systems in providing ancillary grid services by being coordinated with a PU that supplies an AC system's FRR. It is shown that both systems have comparable performance in terms of system dynamic and ensuring the stability of the system providing the FRR, however the VSC technology, featuring a continuous, larger operating range, is capable of providing regulation services at twice the margin of the LCC system.

References

[1] O. E. Oni e I. E. Davidson, "A Review of LCC-HVDC and VSC-HVDC Technologies and Applications", IEEE 16th International Conference on Environment and Electrical Engineering (EEEIC), Florence, Italy, pp. 1-7, 2016.

[2] E. Kimbark, *Direct current transmission*, Volume 1, Portland, Oregon: Wiley-Interscience, 1971.

[3] B. Diban, G. Mazzanti, M. Marzinotto and A. Battaglia, "Life Estimation of HVDC Cables Subjected to Fast and Slow Polarity Reversals", Energies , pp. 17, 3182, 2024.

[4] Terna SpA, Annex A.15 Italian Grid Code: "Partecipazione alla regolazione di Frequenza e Frequenza-Potenza". Terna.it. [Online.] Available: https://www.terna.it/it/sistema-elettrico/codici-rete/codice-rete-italiano. Accessed: Jun. 20, 2025.

[5] Terna SpA, Annex A.79 Italian Grid Code: "Impianti con sistemi di accumulo elettrochimico, Condizioni generali di connessione alle reti AAT e AT". Terna.it. [Online.] Available: https://www.terna.it/it/sistema-elettrico/codici-rete/codice-rete-italiano. Accessed: Jun. 20, 2025.

[6] MATLAB Central File Exchange, "VSC-Based HVDC Link". Mathworks.com. [Online.] Available: https://it.mathworks.com/help/sps/powersys/ug/vsc-based-hvdc-link.html. Accessed: Jun. 20, 2025.

[7] MathWorks, SPS trnasmission and distribution models, examples. Mathworks.com. [Online.] Available: https://it.mathworks.com/help/sps/transmission-and-distribution.html?s_tid=CRUX_lftnav. Accessed: Jun. 20, 2025.

[8] MATLAB Central File Exchange, "Thyristor-Based HVDC Link". Mathworks.com. [Online.] Available: https://it.mathworks.com/help/sps/powersys/ug/thyristor-based-hvdc-link.html. Accessed: Jun. 20, 2025.

[9] ENTSO-E, "HVDC Links in System Operations - Technical Paper". Entso-e.eu. [Online.] Available: https://eepublicdownloads.entsoe.eu/clean-documents/SOC%20documents/20191203_HVDC%20links%20in%20system%20operations.pdf. Accessed: Jun. 20, 2025.